



## Adaptive mesh extended cubic B-spline method for singularly perturbed delay Sobolev problems

Shegaye Lema Cheru, Gemechis File Duressa and Tariku Birabasa Mekonnen

**Abstract.** The purpose of this paper is to develop a robust numerical scheme for a class of singularly perturbed delay Sobolev (pseudo-parabolic) problems that have wide application in various branches of mathematical physics and fluid mechanics. For the small perturbation parameter, the standard numerical schemes for the solution of these problems fail to resolve the boundary layer(s) and the oscillations occur near the boundary layer. Thus, in this paper to resolve the boundary layer(s), implicit Euler scheme for the time derivatives on uniform mesh and extended B-splines basis functions consisting of free parameter  $\lambda$  are presented for spatial variable on Bakhvalov type mesh. The stability and uniform convergence analysis of the proposed method are established. The error estimation of the developed method is shown to be first order accurate in time and second order accurate in space. Numerical experimentation is carried out to validate the applicability of the developed numerical method. The numerical results reveals that the computational result is in agreement with the theoretical estimations.

**Keywords.** Delay partial differential equations, extended B-splines, parameter-uniform convergence, singular perturbation problems, Sobolev problem

### 1 Introduction

The singularly perturbed delay Sobolev problems in the domain  $\bar{D} = \bar{\Omega} \times [0, T], \bar{\Omega} = [0, l], \Omega = (0, l), D = \Omega \times (0, T]$  is the subject of this work. Consider

$$\mathbf{L}u \equiv \mathbf{L}_1 \left[ \frac{\partial u}{\partial t} \right] + \mathbf{L}_2 u(x, t) + c(t)u(x, t - r) = f(x, t), \quad (x, t) \in D, \quad (1.1)$$

with interval and boundary conditions:

$$u(x, t) = \varphi(x, t), \quad (x, t) \in \bar{\Omega} \times [-r, 0], \quad (1.2)$$

$$u(0, t) = u(l, t) = 0, \quad t \in (0, T], \quad (1.3)$$

where

$$\mathbf{L}_1 \left[ \frac{\partial u}{\partial t} \right] \equiv -\varepsilon \frac{\partial^3 u(x, t)}{\partial t \partial x^2} + a(x) \frac{\partial u(x, t)}{\partial t},$$

$$\mathbf{L}_2[u(x, t)] \equiv -\varepsilon \frac{\partial^2 u(x, t)}{\partial x^2} + b(x, t)u(x, t),$$

and  $0 < \varepsilon \ll 1$  small perturbation parameter; the functions  $a, b, c, f$  and  $\varphi$  are sufficiently smooth,  $r > 0$  is delay parameter and  $a(x) \geq \alpha > 0$ .

Sobolev equations are characterized by the occurrence of a time derivative in the highest order term, and many real-world physical problems fall into the category of pseudo-parabolic(Sobolev) problems. They appear in many areas of mathematical physics and fluid dynamics[2], shear in second-order fluids[1, 13], thermodynamics[1], astro-physics[12], filtration theory[19] and propagation of long waves with small amplitude[10]. Some existence and uniqueness results about Sobolev can be found in [13, 14]. The study of Sobolev equations basically began with Sobolev and others in 1950. Much of his work has been motivated by some recent developments in which pseudo-parabolic equations arise in place of the parabolic equations demanded by the classical theories. Nhan[19] have proposed Galerkin approximation technique for nonlinear pseudo-parabolic equations. Amirali[15] considered the  $1 - D$  initial boundary problems for a pseudo-parabolic equation with time delay in second spatial derivative. For a Sobolev problems involving time delay in the  $2nd$ -order derivative, a three layer difference method has been developed in [16]. In [17], a  $1 - D$  delay pseudo-parabolic problem is taken into consideration for numerical solution through the construction of a higher order difference method. Zhang and Tan[18] considered linearized compact finite difference methods(FDMs) for nonlinear Sobolev equations with delay arguments.

Eq. (1.1) is an example of Sobolev equation characterized by having mixed time and space derivatives appearing in the highest order terms. Various types of numerical methods for a parameter free version of initial boundary value problem(IBVP) Eq. (1.1) has been studied by many scholars. There is a scarcity of literature addressing the singularly perturbed nature of the problem described by Eq. (1.1). Duru[6] analyzed Sobolev type equations through a FDM to tackle the boundary layers. Amiraliyev et.al[22] developed a parameter uniform method for IBVP on standard S-mesh on time direction. It is well known that standard discretization methods fail to give accurate results when  $\varepsilon$  is small. Therefore, it is important to develop suitable numerical methods to these problems, whose accuracy does not depend on  $\varepsilon$ .

Many scholars have proposed different numerical methods to solve singularly perturbed Sobolev problems(SPSPs); for instance[3, 6, 22, 23, 24]. But all the mentioned authors considered numerical methods for SPSPs only on interpolating quadrature rules with weight and basis functions. The authors [4, 5] investigated fourth-order SPSPs with time delay. A B-spline collocation method has been developed for time dependent singularly perturbed problems(SPPs) with time lag in [10], parabolic SPPs arising in computational neuro-science in [8] and uniformly convergent collocation method for parabolic SPPs with time delay in[9]. We utilized extended B-spline basis functions on a Bakhvalov mesh to devise a numerical approach for solving SPSPs with large time delay. The adoption of these functions is not as prevalent as other methods such as classical B-splines and FDMs.

Although several works use extended B-splines to build numerical treatments, no paper that addresses numerical approaches for SPSPs with large time delay has been identified, as far as the author is aware. In this study, we utilize the extended B-spline collocation method for the spatial derivative on a Bakhvalov-type mesh and the Implicit Euler scheme for the time derivative on a uniform mesh. One of the key advantages of extended cubic B-splines is their ability to provide a flexible, easiness of the implementation and smooth representation of complex data sets. Despite

this, compared to other approaches like classical B-splines and other methods found in literature, the optimized value of  $\lambda$  yields better accuracy.

This paper is organized as follows: the analytical behavior of Eqs. (1.1)-(1.3) is provided in section 2. The numerical scheme and error bounds for time discretization and spatial discretization using the extended B-spline method on Bakhvalov-type mesh are described in section 3. Section 4 presents the overall error bounds in the spatial direction. Section 5 includes a tabulation of the results from a numerical experiment. The final section offers a conclusion and discusses potential future work.

## 2 Preliminary Results

Here, we deal with the analytical properties of the exact solution, which are needed later in the numerical aspects. If the solution  $u$  of Eq. (1.1) is smooth enough, then the mixed term is written as  $\frac{\partial}{\partial t} \left( \frac{\partial^2 u}{\partial x^2} \right) = \frac{\partial^2}{\partial x^2} \left( \frac{\partial u}{\partial t} \right)$ . Eq. (1.1), in operator form is:

$$\mathbf{L}_\varepsilon u = a(x) \frac{\partial u}{\partial t} - \varepsilon \frac{\partial^3 u}{\partial x^2 \partial t} - \varepsilon \frac{\partial^2 u}{\partial x^2} + b(x, t)u(x, t)$$

**Lemma 2.1.** (*Maximum Principle*) Suppose  $\Phi(x, t) \in C^0(\bar{D}) \cap C^2(D)$ . If  $\Phi(x, t) \geq 0, \forall (x, t) \in \partial D$  and  $\mathbf{L}_\varepsilon \Phi(x, t) \geq 0, \forall (x, t) \in D$ , then  $\Phi(x, t) \geq 0, \forall (x, t) \in \bar{D}$ .

*Proof.* Assume there exists  $(x^*, t^*) \in \bar{D}$  such that  $\Phi(x^*, t^*) = \min_{(x,t) \in \bar{D}} \Phi(x, t) < 0$ . Now,  $(x^*, t^*) \notin \partial D$  and implies that  $(x^*, t^*) \in D$ . Applying the differential operator  $\mathbf{L}_\varepsilon u$  in Eq. (1.1) on  $\Phi(x, t)$  at the critical point  $(x^*, t^*)$  yields

$$\mathbf{L}_\varepsilon \Phi(x^*, t^*) = a(x^*) \frac{\partial \Phi(x^*, t^*)}{\partial t} - \varepsilon \frac{\partial^3 \Phi(x^*, t^*)}{\partial t \partial x^2} - \varepsilon \frac{\partial^2 \Phi(x^*, t^*)}{\partial x^2} + b(x^*, t^*) \Phi(x^*, t^*),$$

By the partial derivative test, we have  $\frac{\partial^2 \Phi(x^*, t^*)}{\partial x^2} \geq 0, \frac{\partial \Phi(x^*, t^*)}{\partial t} = 0$ . Incorporating our assumptions, that  $\Phi(x^*, t^*) \leq 0$ , we can arrive at

$$\mathbf{L}_\varepsilon \Phi(x^*, t^*) = -\varepsilon \frac{\partial^2 \Phi(x^*, t^*)}{\partial x^2} + b(x^*, t^*) \Phi(x^*, t^*) \leq 0.$$

This contradicts the hypothesis. Therefore, we can conclude that the minimum of  $\Phi(x, t)$  is nonnegative(see[21]) and uniqueness of Eq. (1.1) follows from this maximum principle.  $\square$

**Lemma 2.2.** *The solution  $u(x, t)$  of Eqs. (1.1)-(1.3) holds*

$$\varepsilon \left\| \frac{\partial u}{\partial x} \right\|^2 + \alpha \|u\|^2 \leq \left\{ \left[ \varepsilon \left\| \frac{\partial \varphi(x, 0)}{\partial x} \right\|^2 + \|\varphi(x, 0)\|^2 \right] e^{Ct} + \int_0^t c^* \|\varphi(x, s)\|^2 e^{Cs} ds + \int_0^t \|f\|^2 e^{Cs} ds \right\} \quad (2.1)$$

where  $\|\cdot\| = \|\cdot\|_{L_2(0,1)}$  and  $C$  is a generic positive constant.

*Proof.* The proof of Lemma(2.2), Eq. (2.1) is provided in [3, 4, 5, 6, 23, 24].  $\square$

**Lemma 2.3.** *Under the assumption  $a \in C^2[0, l]$ ,  $b \in C_0^2(\overline{D})$ ,  $f \in C(\overline{D})$  and*

$$|a(0) - b(0, t)| \leq C\varepsilon, \quad |a(l) - b(l, t)| \leq C\varepsilon, \quad (2.2)$$

*asymptotic expansion of the solution of Eqs. (1.1)-(1.3) can be written as:*

$$u(x, t) = u_0(x, t) + \vartheta_0(\xi, t) + \omega_0(\eta, t) + \sqrt{\varepsilon} [u_1(x, t) + \vartheta_1(\xi, t) + \omega_1(\eta, t)] + R^*(x, t), \quad (2.3)$$

*where  $u_0(x, t)$  is the solution of reduced problem,  $\vartheta_0(\xi, t)$  and  $\omega_0(\eta, t)$  are functions taking into account the layer behavior of the solution near the points  $x = 0$  and  $x = l$ , respectively and each term in Eq (2.3) are given as follows:*

$$\begin{cases} a(x) \frac{\partial u_0}{\partial t} + b(x, t)u_0 + c(t)u_0(x, t-r) = f(x, t), \\ u_0(x, t-r) = \varphi(x), \quad -r \leq t \leq 0; \end{cases}$$

$$\begin{cases} a(x) \frac{\partial u_1}{\partial t} + b(x, t)u_1 + c(t)u_1(x, t-r) = -\sqrt{\varepsilon} \left[ \frac{\partial^3 u_0}{\partial t \partial x^2} + \frac{\partial^2 u_0}{\partial x^2} \right], \\ u_1(x, t) = 0, \quad -r \leq t \leq 0; \end{cases}$$

$$\begin{cases} -\varepsilon \frac{\partial^3 \vartheta_0}{\partial t \partial \xi^2} + a(0) \frac{\partial \vartheta_0}{\partial t} - \varepsilon \frac{\partial^2 \vartheta_0}{\partial \xi^2} + a(0)\vartheta_0 + c(t)\vartheta_0(x, t-r) = 0, \\ \vartheta_0(\xi, t) = 0, \quad -r \leq t \leq 0; \\ \vartheta_0(0, t) = -u_0(0, t); \quad \vartheta_0(\frac{l}{\sqrt{\varepsilon}}, t) = 0; \end{cases}$$

$$\begin{cases} -\varepsilon \frac{\partial^3 \vartheta_1}{\partial t \partial \xi^2} + a(0) \frac{\partial \vartheta_1}{\partial t} - \varepsilon \frac{\partial^2 \vartheta_1}{\partial \xi^2} + a(0)\vartheta_1 + c(t)\vartheta_1(x, t-r) = -\xi \frac{\partial b(0, t)}{\partial x} \vartheta_0 - \xi a'(0) \frac{\partial \vartheta_0}{\partial t}, \\ \vartheta_1(\xi, t) = 0, \quad -r \leq t \leq 0; \\ \vartheta_1(0, t) = -u_1(0, t); \quad \vartheta_1(\frac{l}{\sqrt{\varepsilon}}, t) = 0; \end{cases}$$

$$\begin{cases} -\varepsilon \frac{\partial^3 \omega_0}{\partial t \partial \eta^2} + a(l) \frac{\partial \omega_0}{\partial t} - \varepsilon \frac{\partial^2 \omega_0}{\partial \eta^2} + a(l)\omega_0 + c(t)\omega_0(x, t-r) = 0, \\ \omega_0(\eta, t) = 0, \quad -r \leq t \leq 0; \\ \omega_0(\frac{l}{\sqrt{\varepsilon}}, t) = 0; \quad \omega_0(0, t) = -u_0(l, t), \end{cases}$$

$$\begin{cases} -\varepsilon \frac{\partial^3 \omega_1}{\partial t \partial \eta^2} + a(l) \frac{\partial \omega_1}{\partial t} - \varepsilon \frac{\partial^2 \omega_1}{\partial \eta^2} + a(l)\omega_1 + c(t)\omega_1(x, t-r) = -\eta \frac{\partial b(l, t)}{\partial x} \omega_0 - \eta a'(l) \frac{\partial \omega_0}{\partial t}, \\ \omega_1(\eta, t) = 0, \quad -r \leq t \leq 0; \\ \omega_0(\frac{l}{\sqrt{\varepsilon}}, t) = 0; \quad \omega_0(0, t) = -u_1(l, t), \end{cases}$$

where  $\xi = \frac{x}{\sqrt{\varepsilon}}$  and  $\eta = \frac{l-x}{\sqrt{\varepsilon}}$ . The remainder term of the asymptotic expansion is:

$$\varepsilon^s \left\| \frac{\partial^{k+s} R^*}{\partial t^k \partial x^s} \right\| \leq C\varepsilon^{1-\frac{s}{2}}, \quad k, s = 0, 1, 2.$$

*Proof.* Similar proof can be found in [4, 5, 23, 24]. □

**Lemma 2.4.** Under the conditions of Eq. (2.2) and  $(x, t) \in \bar{D}$ ,  $k = s = 0, 1, 2$  considering

$$\left| \frac{\partial^{k+s} \vartheta_0}{\partial t^k \partial x^s} \right| \leq C \varepsilon^{-s/2} e^{-x\sqrt{a(0)/\varepsilon}} \quad \text{and} \quad \left| \frac{\partial^{k+s} \omega_0}{\partial t^k \partial x^s} \right| \leq C \varepsilon^{-s/2} e^{-(1-x)\sqrt{a(l)/\varepsilon}},$$

and under the assumption  $f(0, t) = f(l, t) = 0$ , we have the estimate for  $k = s = 0, 1, 2$

$$\left| \frac{\partial^{k+s} u}{\partial t^k \partial x^s} \right| \leq C \left\{ 1 + \varepsilon^{-s/2} \left[ e^{-x\sqrt{a(0)/\varepsilon}} + e^{-(l-x)\sqrt{a(l)/\varepsilon}} \right] \right\}, \quad (x, t) \in \bar{D}. \quad (2.4)$$

*Proof.* For the proof of Lemma (2.4), Eq. (2.4), refer([3, 4, 5, 6]) □

**Remark.** The compatibility conditions at the corner points are given as:

$$\varphi(0, 0) = 0, \quad \varphi(l, 0) = 0, \quad \text{and}$$

$$\begin{cases} -\varepsilon \frac{\partial^2 \varphi(0, 0)}{\partial x^2} + b(0, 0)\varphi(0, 0) = -c(0)\varphi(0, -r) + f(0, 0), \\ -\varepsilon \frac{\partial^2 \varphi(l, 0)}{\partial x^2} + b(l, 0)\varphi(l, 0) = -c(0)\varphi(l, -r) + f(l, 0). \end{cases}$$

Under these assumptions, the IBVP Eq. (1.1)- (1.3) admits a unique solutions.

### 3 Formulation of the Numerical Method

Here, we discretize the temporal and spatial domain of Eq. (1.1)- (1.3) to develop the numerical scheme.

#### 3.1 The Time Semi-discretization

Here we present steps to find interpolating points, which can be used to express  $t - \tau$ ,  $\tau = r$  in terms of grid points, from which  $u(x, t - r)$  can be computed. Now,

1. For a fixed  $M$ , compute  $\bar{\Lambda}^M = \{t_j : t_j = j\Delta t, \quad j = 0, \dots, M\}$  and fix value of  $\tau = r$ .
2.  $u(x, t) = \varphi(x, t)$  for  $-r \leq t \leq 0$ ,  $u(0, t) = u(l, t) = 0$ , from interval and BCs.
3. Compute  $K$  such that  $K = \lfloor \frac{\tau}{\Delta t} \rfloor$ , where  $\lfloor p \rfloor$  is used for the floor of  $p$ .
4. For any  $t_j$  in  $\{t_j\}_{j=1}^K \subset \{t : 0 < t \leq \tau\}$ , it is clear that  $t_j - \tau \in (-\tau, 0]$  and hence  $u(x, t - \tau)$  can be replaced by  $\varphi(x, t - \tau)$ (from the interval condition).
5. For any  $t_j \in \{t_j\}_{j=K+1}^M \subset \{t : \tau < t < 1\}$ , then  $t - \tau \in [t_{j-K-1}, t_{j-K}]$ .

Let  $U^{j+1}(x)$  be the approximation of  $u(x, t_{j+1})$  at  $(j + 1)$ th time level, then introducing the

operator  $D_t^- U^j = \frac{U_i^j - U_i^{j-1}}{\Delta t}$ , we discretize the problem (1.1-1.3) as:

$$\begin{cases} U^{j+1}(x) = \varphi(x, t_{j+1}), & x \in \Omega, -(K+1) \leq j < 0, \\ -\left(\varepsilon + \frac{\varepsilon}{\Delta t}\right) U_{xx}^{j+1}(x) + \left(\frac{a(x)}{\Delta t} + b^{j+1}(x)\right) U^{j+1}(x) = -\frac{\varepsilon}{\Delta t} U_{xx}^j(x) + \\ \frac{a(x)}{\Delta t} U^j(x) - c^{j+1} U^{j-K+1}(x) + f(x, t_{j+1}), & x \in \Omega, 0 \leq j \leq M-1, \\ U^{j+1}(0) = U^{j+1}(l) = 0, & 0 \leq j \leq M. \end{cases} \quad (3.1)$$

Equation (3.1) can be rewritten as

$$\begin{cases} \tilde{L}_\varepsilon U^{j+1}(x) = g^{j+1}(x), & x \in \Omega, 0 \leq j \leq M-1, \\ U^{j+1}(x) = \varphi(x, t_{j+1}), & x \in \Omega, -(K+1) \leq j < 0, \\ U^{j+1}(0) = U^{j+1}(l) = 0, & 0 \leq j \leq M, \end{cases} \quad (3.2)$$

where  $g^{j+1}(x) = -\frac{\varepsilon}{\Delta t} U_{xx}^j(x) + \frac{a(x)}{\Delta t} U^j(x) - c^{j+1} U^{j-K+1}(x) + f(x, t_{j+1})$  and the operator  $\tilde{L}_\varepsilon$  is defined as Eq. (3.3):

$$\tilde{L}_\varepsilon U^{j+1}(x) = -\left(\varepsilon + \frac{\varepsilon}{\Delta t}\right) U_{xx}^{j+1}(x) + \left(\frac{a(x)}{\Delta t} + b^{j+1}(x)\right) U^{j+1}(x). \quad (3.3)$$

The subsequent lemma estimates the bound for local truncation error(LTE), indicating how much each time step contributes to the overall error of the time discretization(see[8]).

**Lemma 3.1.** *If*

$$\left| \frac{\partial^{i+j} u(x, t)}{\partial x^i \partial t^j} \right| \leq C, \quad (x, t) \in [0, l] \times [0, T], \quad 0 \leq j \leq 3, \quad 0 \leq i \leq 3,$$

then the LTE associated to the semi-discrete scheme Eq. (3.2) satisfies

$$\|e_{j+1}\|_\infty \leq C(\Delta t)^2, \quad (3.4)$$

where  $e_{j+1} = u(x, t_{j+1}) - U(x, t_{j+1})$  is the local error estimates in the temporal direction at  $(j+1)$ th time level and the global truncation error at time  $t_{j+1}$  satisfies

$$\|E_j\|_\infty \leq C(\Delta t). \quad (3.5)$$

where  $C$  is constant independent from number of mesh points in time direction.

*Proof.* Since  $U^{j+1}(x)$  satisfies

$$\tilde{L}_\varepsilon U^{j+1}(x) = g^{j+1}(x) \quad (3.6)$$

and solution of Eq. (1.1)- (1.3) is smooth enough, using mean value theorem, we have:

$$\begin{aligned} g^{j+1}(x) &= \tilde{L}_\varepsilon U^{j+1}(x) + \int_{t_j}^{t_{j+1}} (t_j - \varsigma) \frac{\partial^2 u}{\partial t^2}(\varsigma) d\varsigma, \\ &= \tilde{L}_\varepsilon U^{j+1}(x) + O((\Delta t)^2). \end{aligned} \quad (3.7)$$

From Eq. (3.6)- (3.7), the LTE corresponding to Eq. (3.1) is given by  $e_{j+1} = u(x, t_{j+1}) - U(x, t_{j+1})$  and satisfy the boundary value problem:

$$\tilde{L}_\varepsilon e_{j+1} = O((\Delta t)^2) \Rightarrow e_{j+1} = \left(\tilde{L}_\varepsilon u\right)^{-1} O((\Delta t)^2), \quad e_{j+1}(0) = e_{j+1}(l) = 0. \quad (3.8)$$

An application of maximum principle on operator  $\tilde{L}_\varepsilon u$  and Eq. (3.8) gives:

$$\|e_{j+1}\|_\infty \leq C(\Delta t)^2.$$

The LTE given in Eq. (3.4) measures the contributions of each time step to the global error of time discretization. The global error estimate(Eq. (3.5)) at the  $j$ th time step is

$$\begin{aligned} \|E_j\|_\infty &= \left\| \sum_{i=1}^{j-1} e_i \right\|_\infty, \quad (j) \leq \frac{T}{\Delta t}, \\ &\leq \|e_1\|_\infty + \|e_2\|_\infty + \dots + \|e_{j-1}\|_\infty, \\ &\leq C((j)k)(\Delta t)^2 \leq C(j\Delta t)(\Delta t) \leq C_1 T(\Delta t) \leq C_1 T(\Delta t) \leq C_3(\Delta t). \end{aligned}$$

where  $C_1$  is a positive constant independent of  $\varepsilon$  and  $\Delta t$ . □

## 3.2 The spatial discretization

To discretize space variable, layer adapted meshes called Bakhvalov mesh is presented.

### 3.2.1 The Mesh Generation

In this section, we construct Bakhvalov mesh that generates more mesh points in the layer region than in the other part of the domain. We divide the three non overlapping subintervals  $[0, \sigma_1]$ ,  $[\sigma_1, \sigma_2]$  and  $[\sigma_2, l]$  into  $N/4$ ,  $N/2$  and  $N/4$  equidistant subintervals respectively. The transition point is taken as:

$$\sigma_1 = \min \left\{ \frac{l}{4}, \alpha^{-1} \varepsilon |\ln \varepsilon| \right\}, \quad \sigma_2 = l - \sigma_1. \quad (3.9)$$

Moreover, using Eq. (3.9)  $x_i$ , node points are specified as(see [23, 24]):

$$x_i = \begin{cases} -\alpha^{-1} \varepsilon \ln \left( 1 - (1 - \varepsilon) \frac{4i}{N} \right), & i = 0(1) \frac{N}{4}, x_i \in [0, \sigma_1], \sigma_1 < \frac{l}{4}; \\ -\alpha^{-1} \varepsilon \ln \left( 1 - (1 - e^{-\alpha l/4\varepsilon}) \frac{4i}{N} \right), & i = 0(1) \frac{N}{4}, x_i \in [0, \sigma_1], \sigma_1 = \frac{l}{4}; \\ \sigma_1 + \left( i - \frac{N}{4} \right) \frac{2(\sigma_2 - \sigma_1)}{N}, & i = \frac{N}{4} + 1(1) \frac{3N}{4}, x_i \in [\sigma_1, \sigma_2]; \\ \sigma_2 - \alpha^{-1} \varepsilon \ln \left( 1 - (1 - \varepsilon) \frac{4 \left( i - \frac{3N}{4} \right)}{N} \right), & i = \frac{3N}{4} + 1(1)N, x_i \in [\sigma_2, l], \sigma_2 < \frac{3l}{4}; \\ \sigma_2 - \alpha^{-1} \varepsilon \ln \left( 1 - (1 - e^{-\alpha l/4\varepsilon}) \frac{4 \left( i - \frac{3N}{4} \right)}{N} \right), & i = \frac{3N}{4} + 1(1)N, x_i \in [\sigma_2, l], \sigma_2 = \frac{3l}{4}. \end{cases} \quad (3.10)$$

### 3.2.2 Extended B-spline Collocation Method

Let  $x_i : 0 = x_0 < \dots < x_N = l$  be the spatial domain  $[0, l]$  with non-uniform mesh spacing  $h_i = x_i - x_{i-1}$  which is given in Eq. (3.10). The extended form of B-spline of degree 4,  $Q_i(x, \lambda)$ ,  $i =$

$-1, 0, \dots, N + 1$ , is defined by[8, 9, 10],

$$Q_i(x, \lambda) = \frac{1}{24h_i^2} \begin{cases} 4h_i(1 - \lambda)(x - x_{i-2})^3 + 3\lambda(x - x_{i-2})^4, & \text{if } [x_{i-2}, x_{i-1}], \\ (4 - \lambda)h_i^4 + 12h_i^3(x - x_{i-1}) + 6h_i^2(2 + \lambda)(x - x_{i-1})^2 - \\ \quad 12h_i(x - x_{i-1})^3 - 3\lambda(x - x_{i-1})^4, & \text{if } [x_{i-1}, x_i], \\ (4 - \lambda)h_i^4 + 12h_i^3(x_{i+1} - x) + 6h_i^2(2 + \lambda)(x_{i+1} - x)^2 - \\ \quad 12h_i(x_{i+1} - x)^3 - 3\lambda(x_{i+1} - x)^4, & \text{if } [x_i, x_{i+1}], \\ 4h_i(1 - \lambda)(x_{i+2} - x)^3 + 3\lambda(x_{i+2} - x)^4, & \text{if } [x_{i+1}, x_{i+2}], \\ 0, & \text{otherwise.} \end{cases} \tag{3.11}$$

The extended B-splines and its first four derivatives vanish outside the region  $x_{i-2}, x_{i+2}$  and  $-m(m - 2) \leq \lambda \leq 1$  is a free parameter which is used to change the shape of extended cubic B-splines functions. The variation in  $m$  gives different forms of extended cubic B-splines functions. The extended cubic B-spline function has one free parameter  $\lambda$ , which controls tension of the solution curve and when  $\lambda \rightarrow 0$ , the extended cubic B-spline reduced to convectional cubic B-spline functions. For  $\lambda \in [-8, 1]$ , cubic B-spline and extended cubic B-spline share the same properties. Since, B-spline of degree  $p$  are  $(p - 1)$  continuously differentiable piecewise polynomials that forms a basis of splines, let  $\Xi_3(\Omega) \subset C^2(\Omega)$ . Since each  $Q_i(x)$  is also a piecewise cubic with knots at  $\Omega$ , each  $Q_i(x) \in \Xi_3(\Omega)$ . Suppose that  $Q_3(\Omega) = span \{Q_{-1}, Q_0, \dots, Q_N, Q_{N+1}\}$ . Since, the functions  $Q_i$ 's are linearly independent on  $[0, l]$ ,  $Q_3(\Omega)$  is an  $(N + 3)$  dimensional. The value of extended B-splines and its derivatives at the nodal points can be calculated from Eq. (3.11) and depicted in Table. (1).

Table 1: Values of  $Q_i(x, \lambda), Q_i'(x, \lambda)$  and  $Q_i''(x, \lambda)$  at nodal points

	$x_{i-2}$	$x_{i-1}$	$x_i$	$x_{i+1}$	$x_{i+2}$
$Q_i(x, \lambda)$	0	$\frac{4-\lambda}{24}$	$\frac{8+\lambda}{12}$	$\frac{4-\lambda}{24}$	0
$Q_i'(x, \lambda)$	0	$\frac{1}{2h_i}$	0	$-\frac{1}{2h_i}$	0
$Q_i''(x, \lambda)$	0	$\frac{2+\lambda}{2h_i^2}$	$-\frac{2+\lambda}{h_i^2}$	$\frac{2+\lambda}{2h_i^2}$	0

Let  $S(x, \lambda)$  be the B-spline interpolating function for  $U(x, t)$  at the nodal points and  $S(x, \lambda) \in Q_3(\Omega)$ . We aim to find an approximate solution, denoted as  $S(x, \lambda)$ , to the problem described by Eq. (3.1) through (3.2). This solution is expressed as:

$$S(x, \lambda) = \sum_{i=-1}^{N+1} \gamma_i Q_i(x, \lambda), \tag{3.12}$$

where  $\gamma_i$  are unknown real coefficients to be determined by requiring that  $S(x, \lambda)$  satisfies Eq. (3.2) at  $(N + 1)$  collocation points and BCs. Using Eq. (3.12) and Table (1),  $S_i(x, \lambda)$  and its derivatives at the knots are determined in terms of the parameters as follows:

$$\begin{cases} S_i(x, \lambda) = \frac{4-\lambda}{24} \gamma_{i-1} + \frac{8+\lambda}{12} \gamma_i + \frac{4-\lambda}{24} \gamma_{i+1}, \\ S_i'(x, \lambda) = \frac{1}{2h_i} \gamma_{i+1} - \frac{1}{2h_i} \gamma_{i-1}, \\ S_i''(x, \lambda) = \frac{2+\lambda}{2h_i^2} \gamma_{i-1} - \frac{2+\lambda}{h_i^2} \gamma_i + \frac{2+\lambda}{2h_i^2} \gamma_{i+1}. \end{cases} \tag{3.13}$$

We determine the values of  $\gamma_i$ 's and thus the approximation to the solution of BVP, by selecting collocation points to coincide with nodes and then substituting the approximate solution  $S_i(x, \lambda)$

and its derivatives Eq. (3.13) at the knots into Eq. (3.2), we obtain  $(N + 1)$  linear equations in  $(N + 3)$  unknowns.

$$r_i^- \gamma_{i-1}^{j+1} + r_i^c \gamma_i^{j+1} + r_i^+ \gamma_{i+1}^{j+1} = E_i^- \gamma_{i-1}^j + E_i^c \gamma_i^j + E_i^+ \gamma_{i+1}^j + \tilde{G}_i, \quad \text{for } i = 0(1)N, \quad (3.14)$$

where the coefficients are given by:

$$\begin{cases} r_i^- = -\varepsilon \left( \frac{2+\lambda}{2h_i^2} + \frac{2+\lambda}{2\Delta t h_i^2} \right) + \frac{a_i(4-\lambda)}{24\Delta t} + \frac{b_i^{j+1}(4-\lambda)}{24}, \\ r_i^c = \varepsilon \left( \frac{2+\lambda}{h_i^2} + \frac{2+\lambda}{\Delta t h_i^2} \right) + \frac{a_i(8+\lambda)}{12\Delta t} + \frac{b_i^{j+1}(8+\lambda)}{12}, \\ r_i^+ = -\varepsilon \left( \frac{2+\lambda}{2h_i^2} + \frac{2+\lambda}{2\Delta t h_i^2} \right) + \frac{a_i(4-\lambda)}{24\Delta t} + \frac{b_i^{j+1}(4-\lambda)}{24}, \\ E_i^- = -\varepsilon \frac{2+\lambda}{2\Delta t h_i^2} + \frac{a_i(4-\lambda)}{24\Delta t}, \quad E_i^c = \varepsilon \frac{2+\lambda}{\Delta t h_i^2} + \frac{a_i(8+\lambda)}{12\Delta t}, \\ E_i^+ = -\varepsilon \frac{2+\lambda}{2\Delta t h_i^2} + \frac{a_i(4-\lambda)}{24\Delta t}, \quad \tilde{G}_i = f_i^{j+1} - c^{j+1} U_i^{j-K+1}. \end{cases} \quad (3.15)$$

### Imposing Boundary conditions

BCs in Eq. (3.2) at  $x_0 = 0$  and  $x_N = N$  must be imposed to the system in Eq. (3.14) to obtain the unique solution. Thus, the approximate solution at two boundary points is:

$$\begin{cases} \gamma_{-1}^{j+1} = -2 \frac{(8+\lambda)}{4-\lambda} \gamma_0^{j+1} - \gamma_1^{j+1}, \quad \text{for } i = 0. \\ \gamma_{N+1}^{j+1} = -\gamma_{N-1}^{j+1} - 2 \frac{(8+\lambda)}{4-\lambda} \gamma_N^{j+1}, \quad \text{for } i = N. \end{cases} \quad (3.16)$$

Thus, Eq. (3.14) and Eq. (3.16) lead to  $(N + 3) \times (N + 3)$  system with  $(N + 3)$  unknowns. Now by substituting Eq. (3.16) in Eq. (3.14), we obtain

$$\begin{aligned} \left( r_0^c - 2r_0^- \frac{8+\lambda}{4-\lambda} \right) \gamma_0^{j+1} + (r_0^+ - r_0^-) \gamma_1^{j+1} = \\ \left( E_0^c - 2E_0^- \frac{8+\lambda}{4-\lambda} \right) \gamma_0^j + (E_0^+ - E_0^-) \gamma_1^j + \tilde{G}_0^{j+1}, \quad i = 0. \end{aligned} \quad (3.17)$$

$$\begin{aligned} (r_N^- - r_N^+) \gamma_{N-1}^{j+1} + \left( r_N^c - 2r_N^+ \frac{8+\lambda}{4-\lambda} \right) \gamma_N^{j+1} = \\ (E_N^- - E_N^+) \gamma_{N-1}^j + \left( E_N^c - 2E_N^+ \frac{8+\lambda}{4-\lambda} \right) \gamma_N^j + \tilde{G}_N^{j+1}, \quad i = N. \end{aligned} \quad (3.18)$$

Now, Eq. (3.14)- (3.18) lead to  $(N + 3) \times (N + 3)$  linear system with  $(N + 3)$  unknowns  $\gamma_{-1}, \gamma_0, \dots, \gamma_N, \gamma_{N+1}$ . Excluding the unknowns  $\gamma_{-1}$  and  $\gamma_{N+1}$  from Eq. (3.17) and Eq. (3.18) for  $i = 0$  and  $i = N$ , then Eq. (3.14) becomes solvable  $(N + 1) \times (N + 1)$  system of linear equations in  $(N + 1)$  unknowns  $\gamma_0, \gamma_1, \dots, \gamma_{N-1}, \gamma_N$ , in matrix form as

$$M \gamma_i^{j+1} = N \gamma_i^j + G, \quad i = 1, 2, \dots, N - 1, \quad (3.19)$$

where the entries of the tridiagonal matrix  $M = m_{ij}$  and  $N = n_{ij}$  are given as:

$$M = \begin{bmatrix} \left(r_0^c - 2r_0^- \frac{8 + \lambda}{4 - \lambda}\right) & (r_0^+ - r_0^-) & 0 & 0 & \dots & 0 & 0 & 0 \\ r_1^- & r_1^c & r_1^+ & 0 & \dots & 0 & 0 & 0 \\ 0 & r_2^- & r_2^c & r_2^+ & \dots & 0 & 0 & 0 \\ \vdots & \vdots & \vdots & \vdots & \dots & \vdots & \vdots & \vdots \\ 0 & 0 & 0 & 0 & \dots & r_{N-1}^- & r_{N-1}^c & r_{N-1}^+ \\ 0 & 0 & 0 & 0 & \dots & 0 & (r_N^- + r_N^+) & \left(r_N^c - 2r_N^+ \frac{8 + \lambda}{4 - \lambda}\right) \end{bmatrix}$$

$$N = \begin{bmatrix} \left(E_0^c - 2E_0^- \frac{8 + \lambda}{4 - \lambda}\right) & (E_0^+ - E_0^-) & 0 & \dots & 0 & 0 & 0 & 0 \\ E_1^- & E_1^c & E_1^+ & \dots & 0 & 0 & 0 & 0 \\ \vdots & \vdots \\ 0 & 0 & 0 & \dots & E_{N-1}^- & E_{N-1}^c & E_{N-1}^+ & 0 \\ 0 & 0 & 0 & \dots & 0 & (E_N^- + E_N^+) & \left(E_N^c - 2E_N^+ \frac{8 + \lambda}{4 - \lambda}\right) & 0 \end{bmatrix}$$

The entries of column vector  $\gamma$  are  $\gamma = (\gamma_0, \dots, \gamma_{N-1}, \gamma_N)^T$  and column vector  $G$  is

$$G = \begin{cases} \tilde{G}_0^{j+1}, & j = 0, \\ \tilde{G}_i^{j+1}, & j = 1(1)M - 1, \\ \tilde{G}_N^{j+1}, & j = N. \end{cases} \tag{3.20}$$

Now, Eq. (3.19- 3.20) can be rewritten as:

$$M\gamma_i^{j+1} = H_i, \quad \text{where,} \quad H_i = N\gamma_i^j + G, \tag{3.21}$$

The matrix  $M$  in Eq. (3.21) is strictly diagonally dominant as they satisfy the relations

$$|a_{i,j}| - (|a_{i,j-1}| + |a_{i,j+1}|) = \frac{a_i}{12\Delta t} (4 + 2\lambda) > 0,$$

since  $a_i \geq \alpha > 0$ , we observe that for  $\lambda > -2$ , the matrix  $M$  is strictly diagonally dominant and hence non-singular. For a matrix  $M$  which is diagonally dominant both rows and by columns, we give bounds for  $\|M^{-1}\|_1$  and  $\|M^{-1}\|_\infty$ , which can be used to give a lower bound for the smallest singular value. If  $M$  is diagonally dominant by rows (i.e.,  $|a_{kk}| > \sum_{j \neq k} |a_{kj}|, 1 \leq k \leq n$ ), we can bound the  $L_\infty$  norm of  $M^{-1}$  by the following lemma:

**Lemma 3.2.** Assume  $M$  is diagonally dominant by rows and set

$$\nu = \min_k \left( |a_{kk}| - \sum_{j \neq k} |a_{kj}| \right), \quad \text{then} \quad \|M^{-1}\|_\infty \leq \frac{1}{\nu}$$

Therefore, we can solve the linear system Eq. (3.19) uniquely for real unknowns  $(\gamma_0, \gamma_1, \dots, \gamma_{N-1}, \gamma_N)$  by an existing algorithm to solve tridiagonal system and then using BCs Eq. (3.17) and Eq. (3.18), we obtain  $\gamma_{-1}$  and  $\gamma_{N+1}$ . Hence, the method of collocation using a basis of extended cubic B-splines applied to Eq. (3.2) produces a unique approximate solution  $S(x, \lambda)$  at  $(j + 1)th$  time level. The obtained values of  $\gamma'_i s$  are substituted in Eq. (3.12), which is the approximated solution to Eq. (3.2). However, these solution has two free parameter  $x$  and  $\lambda$ . Now to get the better approximation the optimization of  $\lambda$  is required. Once the optimized value of  $\lambda$  is obtained, it will be substituted back and hence the better approximated solution is obtained.

## 4 Parameter Uniform Convergence Analysis

For the derivation of the uniform convergence, we use the following lemmas:

**Lemma 4.1.** *The extended cubic B-splines  $Q_{-1}(x, \lambda), Q_0(x, \lambda), \dots, Q_{N-1}(x, \lambda), Q_N(x, \lambda)$  defined in Eq. (3.11) satisfies the following inequality*

$$\sum_{i=-1}^{N+1} |Q_i(x, \lambda)| \leq \frac{7}{4}, \quad x \in [0, l] \quad (4.1)$$

*Proof.* For the proof of Lemma (4.1) and Eq. (4.1), refer to a series of papers[9, 10].  $\square$

Let  $Y(x)$  be the unique cubic spline interpolate from an approximate solution  $S(x, \lambda)$  of Eq. (3.2) to the solution  $u(x, t)$  which is given by

$$Y(x) = \sum_{i=-1}^{N+1} \bar{\gamma}_i Q_i(x, \lambda) \quad (4.2)$$

**Lemma 4.2.** *Let  $Y(x) \in C^2([0, l])$  given in Eq. (4.2) be the cubic spline interpolant associated with a solution  $\tilde{u}(x)$ . If  $\tilde{u}(x) \in C^4([0, l])$ , it follows from the estimate of Hall[11] that the standard cubic spline interpolation error estimate holds, for  $x \in [x_i, x_{i+1}] \in \Omega$*

$$\left\| D^{(n)} (\hat{u}(x) - Y(x)) \right\| \leq \lambda_n \left\| u^{(4)}(x) \right\| h_i^{4-n}, \quad n = 0, 1, 2, 3, \quad (4.3)$$

where  $\lambda_n$  are constant independent of  $h_i$  and  $N$ .

**Theorem 4.1.** *Let  $S(x, \lambda)$  be an extended cubic B-spline collocation approximation from the space of extended B-splines  $\Xi_3(\Omega)$  to the solution of Eq. (3.2) and  $\hat{u}(x_i)$  is the analytical solution to the problem. If  $\tilde{g}(x) \in C^2([0, l])$ , then the parameter uniform error estimate satisfies the bound*

$$\sup_{0 < \varepsilon \leq 1} \max_{0 \leq i \leq N} \|\hat{u}(x_i) - S(x_i, \lambda)\| \leq CN^{-2}. \quad (4.4)$$

where  $C$  is a constant independent of  $\varepsilon$  and  $N$ .

*Proof.* To estimate the error  $|\hat{u}(x_i) - S(x_i, \lambda)|$ , we use Lemma (2.4,4.2) and Eq. (4.3) as follows:

$$\begin{aligned} & \left| \tilde{L}_\varepsilon \hat{u}(x_i) - \tilde{L}_\varepsilon Y(x_i) \right| \leq \\ & \quad \varepsilon (|\varrho| |\hat{u}''(x_i) - Y''(x_i)|) + |p(x_i)| |\hat{u}(x_i) - Y(x_i)|, \\ & \quad \leq \varepsilon \left( |\varrho| \lambda_2 \left| u^{(4)} \right| h_i^2 \right) + \|p\|_\infty \lambda_0 \left| u^{(4)} \right| h_i^4 \\ & \quad \leq (\varepsilon |\varrho| \lambda_2 h_i^2 + \|p\|_\infty \lambda_0 h_i^4) \left| u^{(4)} \right|, \\ & \quad \leq C \left( (\varepsilon |\varrho| \lambda_2 h_i^2 + \|p\|_\infty \lambda_0 h_i^4) \left( 1 + \varepsilon^{-2} \left[ e^{-x_i \sqrt{(a(0))/\varepsilon}} + e^{-(l-x_i) \sqrt{(a(l))/\varepsilon}} \right] \right) \right), \end{aligned} \quad (4.5)$$

where  $\varrho = (1 + 1/\Delta t)$  and  $p(x_i) = (a_i/\Delta t + b_i^{j+1})$ . Now depending on the magnitude of  $\sigma_1$  and  $\sigma_2$  there arises the following cases:

Case 1. Consider  $\sigma_1 = l/4$  and  $\sigma_2 = 3l/4$ , and so,  $\frac{l}{4} < \alpha_0^{-1}\varepsilon \ln \varepsilon$  and  $\frac{3l}{4} > l - \alpha_0^{-1}\varepsilon \ln \varepsilon$ ,  $h^{(1)} = h^{(2)} = h^{(3)} = lN^{-1}$ . Since

$$\begin{aligned} h_i^{(1)} &= x_i - x_{i-1} \\ &= \alpha^{-1}\varepsilon \left[ \ln \left( 1 - \left( 1 - e^{-\frac{\alpha l}{4\varepsilon}} \right) \frac{4(i-1)}{N} \right) - \ln \left( 1 - \left( 1 - e^{-\frac{\alpha l}{4\varepsilon}} \right) \frac{4(i)}{N} \right) \right], \\ &\leq \alpha^{-1}\varepsilon \left[ \left( 1 - \left( 1 - e^{-\frac{\alpha l}{4\varepsilon}} \right) \frac{4(i-1)}{N} - 1 \right) - \left( 1 - \left( 1 - e^{-\frac{\alpha l}{4\varepsilon}} \right) \frac{4(i)}{N} - 1 \right) \right], \\ &= \alpha^{-1}\varepsilon \left[ - \left( 1 - e^{-\frac{\alpha l}{4\varepsilon}} \right) \frac{4(i-1)}{N} + \left( 1 - e^{-\frac{\alpha l}{4\varepsilon}} \right) \frac{4(i)}{N} \right], \\ &= \alpha^{-1}\varepsilon \left( 1 - e^{-\frac{\alpha l}{4\varepsilon}} \right) \frac{4}{N} \leq 4\alpha^{-1}\varepsilon N^{-1} \leq 4\alpha^{-1}N^{-1} \leq CN^{-1}. \end{aligned}$$

Now,  $\frac{l}{4} < \alpha_0^{-1}\varepsilon \ln \varepsilon \Rightarrow \varepsilon^{-1} \leq 4\alpha^{-1}l^{-1} \ln \varepsilon \leq C \ln \varepsilon$ . Using this and Eq. (4.5), we have

$$\begin{aligned} \left| \tilde{L}_\varepsilon \hat{u}(x_i) - \tilde{L}_\varepsilon Y(x_i) \right| &\leq (\varepsilon |\varrho| \lambda_2 h_i^2 + \|p\|_\infty \lambda_0 h_i^4) |u^{(4)}|, \\ &\leq C\varepsilon^{-2} ((\varepsilon |\varrho| \lambda_2 N^{-2} + \|p\|_\infty \lambda_0 N^{-4})) \\ &\leq CN^{-2} (\varepsilon^{-1} + \varepsilon^{-2} N^{-2}) \\ &\leq CN^{-2} (C \ln \varepsilon + (C \ln \varepsilon)^2 N^{-2}) \\ &\leq CN^{-2}, \quad \text{since } C \ln \varepsilon + (C \ln \varepsilon)^2 N^{-2} \leq C \end{aligned} \tag{4.6}$$

Now for  $\sigma_2 = \frac{3l}{4}$ ,  $\sigma_2 = l - \sigma_1 = \frac{3l}{4}$ ,  $x_i \in [\sigma_2, l]$ ,  $i = 3N/4 + 1, \dots, N$ , we have

$$\begin{aligned} h_i^{(2)} &= x_i - x_{i-1} \\ &= \alpha^{-1}\varepsilon \left[ \ln \left( 1 - \left( 1 - e^{-\frac{\alpha l}{4\varepsilon}} \right) \frac{4(i-1-\frac{3N}{4})}{N} \right) - \ln \left( 1 - \left( 1 - e^{-\frac{\alpha l}{4\varepsilon}} \right) \frac{4(i-\frac{3N}{4})}{N} \right) \right], \\ &\leq \alpha^{-1}\varepsilon \left[ \left( 1 - \left( 1 - e^{-\frac{\alpha l}{4\varepsilon}} \right) \frac{4(i-1-\frac{3N}{4})}{N} - 1 \right) - \left( 1 - \left( 1 - e^{-\frac{\alpha l}{4\varepsilon}} \right) \frac{4(i-\frac{3N}{4})}{N} - 1 \right) \right], \\ &= \alpha^{-1}\varepsilon \left[ - \left( 1 - e^{-\frac{\alpha l}{4\varepsilon}} \right) \frac{4(i-1-\frac{3N}{4})}{N} + \left( 1 - e^{-\frac{\alpha l}{4\varepsilon}} \right) \frac{4(i-\frac{3N}{4})}{N} \right], \\ &= \alpha^{-1}\varepsilon \left( \frac{4}{N} \left( 1 - e^{-\frac{\alpha l}{4\varepsilon}} \right) \right) \leq 4\alpha^{-1}\varepsilon N^{-1} \leq CN^{-1}. \end{aligned}$$

By using  $h_i^{(2)} \leq CN^{-1}$  and Eq. (4.5), we have the following estimate:

$$\left| \tilde{L}_\varepsilon \hat{u}(x_i) - \tilde{L}_\varepsilon Y(x_i) \right| \leq CN^{-2}. \tag{4.7}$$

Case 2. If  $\Omega_i$  lies in the boundary layer regions

1. If  $\sigma_1 < \frac{l}{4}$ ,  $x_i \in [0, \sigma_1]$ ,  $i = 1, \dots, N/4$ , then the mesh spacing is given as:

$$h_i = x_i - x_{i-1} = -\alpha^{-1}\varepsilon \ln \left( 1 - (1 - \varepsilon) \frac{4i}{N} \right) + \alpha^{-1}\varepsilon \ln \left( 1 - (1 - \varepsilon) \frac{4(i-1)}{N} \right),$$

If the mean value theorem[25] is applied to this, we have

$$h_i = 4\alpha^{-1}(1 - \varepsilon)N^{-1} \leq C(1 - \varepsilon)N^{-1}.$$

Using the bound in the layer regions together with Eq. (4.5), we have

$$\left| \tilde{L}_\varepsilon \hat{u}(x_i) - \tilde{L}_\varepsilon Y(x_i) \right| \leq CN^{-2}. \quad (4.8)$$

2. If  $x_i \in [\sigma_1, \sigma_2]$ ,  $x_i = \sigma_1 + \left(i - \frac{N}{4}\right)h^{(1)}$ ,  $i = \frac{N}{4} + 1, \dots, \frac{3N}{4}$ ,  $h^{(1)} = 2\frac{\sigma_2 - \sigma_1}{N}$ , then, the mesh spacing is given as:

- (a) If  $x_i \in [\sigma_1, \sigma_2]$  and  $\sigma_1 = -\alpha^{-1}\varepsilon \ln \varepsilon < \frac{l}{4}$ , then

$$h_i = x_i - x_{i-1} = \sigma_1 + \left(i - \frac{N}{4}\right)h^{(1)} - \sigma_1 - \left(i-1 - \frac{N}{4}\right)h^{(1)} \leq CN^{-1}$$

- (b) If  $x_i \in [\sigma_1, \sigma_2]$  and  $\sigma_1 = \frac{l}{4}$ , then

$$h_i = x_i - x_{i-1} = \sigma_1 + \left(i - \frac{N}{4}\right)h^{(1)} - \sigma_1 - \left(i-1 - \frac{N}{4}\right)h^{(1)} \leq CN^{-1}$$

Now combining this two cases with Eq. (4.5), we get

$$\left| \tilde{L}_\varepsilon \hat{u}(x_i) - \tilde{L}_\varepsilon Y(x_i) \right| \leq CN^{-2}. \quad (4.9)$$

3. If  $x_i \in [\sigma_2, l]$ ,  $x_i = \sigma_2 - \alpha^{-1}\varepsilon \ln \left( 1 - \left( 1 - e^{-\frac{\alpha l}{4\varepsilon}} \right) \frac{4(i - \frac{3N}{4})}{N} \right)$ ,  $i = 3N/4 + 1, \dots, N$ , then the mesh spacing is given as:

$$h_i = x_i - x_{i-1} = \sigma_2 - \alpha^{-1}\varepsilon \ln \left( 1 - \left( 1 - e^{-\frac{\alpha l}{4\varepsilon}} \right) \frac{4(i - \frac{3N}{4})}{N} \right) - \sigma_2 - \alpha^{-1}\varepsilon \ln \left( 1 - \left( 1 - e^{-\frac{\alpha l}{4\varepsilon}} \right) \frac{4(i-1 - \frac{3N}{4})}{N} \right)$$

If the mean value theorem[25] is applied in the above equation, we have

$$h_i = \alpha^{-1}\varepsilon \frac{4(1 - \varepsilon)N^{-1}}{1 - i_1 4(1 - \varepsilon)N^{-1}} \leq 4\alpha^{-1}(1 - \varepsilon)N^{-1} \leq C(1 - \varepsilon)N^{-1}.$$

Now, using this and the estimate in Eq. (4.5), we get

$$\left| \tilde{L}_\varepsilon \hat{u}(x_i) - \tilde{L}_\varepsilon Y(x_i) \right| \leq CN^{-2}. \quad (4.10)$$

Finally, on combining Eq. (4.5) and Eq. (4.6)- (4.10), the estimates holds for all cases:

$$\left| \tilde{L}_\varepsilon \hat{u}(x_i) - \tilde{L}_\varepsilon Y(x_i) \right| \leq CN^{-2}. \quad (4.11)$$

Hence, by combining Eq. (4.6- 4.11), we obtain:

$$\begin{aligned} \left| \tilde{L}_\varepsilon S(x_i) - \tilde{L}_\varepsilon Y(x_i) \right| &= \left| g(x_i, t_{j+1}) - \tilde{L}_\varepsilon Y(x_i) \right| \\ &= \left| \tilde{L}_\varepsilon \hat{u}(x_i) - \tilde{L}_\varepsilon Y(x_i) \right| \leq CN^{-2} |\ln \varepsilon| \leq CN^{-2}. \end{aligned} \quad (4.12)$$

We know that  $\tilde{L}_\varepsilon U(x_i) = \tilde{g}(x_i)$ ,  $0 \leq i \leq N$  with given BCs leads to the linear system  $M\gamma = H$ . Assume that  $\tilde{L}_\varepsilon Y(x_i) = \tilde{g}(x_i)$ ,  $0 \leq i \leq N$  with BCs  $Y(0, t_{j+1}) = Y(l, t_{j+1}) = 0$  leads to the linear system  $M\bar{\gamma} = \bar{H}$ . It follows that:

$$M(\gamma - \bar{\gamma}) = (H - \bar{H}), \quad (4.13)$$

where  $\gamma - \bar{\gamma} = (\gamma_0 - \bar{\gamma}_0, \gamma_1 - \bar{\gamma}_1, \dots, \gamma_N - \bar{\gamma}_N)^T$  and

$$H - \bar{H} = (\tilde{g}(x_0) - \bar{g}(x_0), \tilde{g}(x_1) - \bar{g}(x_1), \dots, \tilde{g}(x_N) - \bar{g}(x_N))^T.$$

Since  $M(\gamma - \bar{\gamma}) = (H - \bar{H})$  implies that  $\tilde{L}_\varepsilon S(x_i) - \tilde{L}_\varepsilon Y(x_i)$ , from Eq. (4.12), we have that

$$\|H - \bar{H}\| \leq CN^{-2} |\ln \varepsilon| \quad (4.14)$$

It can be seen that for  $\lambda > -2$  and reasonable large  $N$  the matrix  $M$  is strictly diagonally dominant and thus nonsingular. From the estimate in Lemma (3.2), we get

$$\|M^{-1}\| \leq C \quad (4.15)$$

Combining this bounds in Eq. (4.13)- (4.15), we obtain

$$\|\gamma - \bar{\gamma}\| \leq CN^{-2} |\ln \varepsilon|. \quad (4.16)$$

Let  $z = (z_0, z_1, \dots, z_N)^T$ , where  $z_i = \gamma_i - \bar{\gamma}_i$ . Now, from Eq. (4.13), we have

$$z = M^{-1} (H - \bar{H}). \quad (4.17)$$

Using Eq. (4.14) and Eq. (4.15) in Eq. (4.17), we have the following estimate:

$$\|z\| \leq CN^{-2} |\ln \varepsilon| \leq CN^{-2}. \quad (4.18)$$

Also the boundary conditions given in Eq. (3.17) and Eq. (3.18) is also bounded by  $CN^{-2} |\ln \varepsilon|$ . Therefore, we are enabled to estimate  $|S(x, \lambda), Y(x)|$  as

$$|S(x, \lambda) - Y(x)| = \sum_{i=-1}^{N+1} (\gamma_i - \bar{\gamma}_i) Q_i(x, \lambda) \quad (4.19)$$

Using Eq. (4.16-4.19) and lemma (4.1), we have

$$\max_{0 \leq i \leq N} |S(x_i, \lambda) - Y(x_i)| \leq CN^{-2}. \quad (4.20)$$

Hence, we arrive at Theorem (4.1) and Eq. (4.4), which completes the proof.  $\square$

**Theorem 4.2.** Let  $S(x_i, \lambda)$  be the extended B-spline collocation approximation to the solution  $u(x, t)$  of Eq. (4.17) at  $(j + 1)$ th time level. Then, the parameter-uniform error estimates of the fully discrete scheme is given by

$$|u(x_i) - S(x_i, \lambda)| \leq C (\Delta t + N^{-2}), \quad 0 \leq i \leq N \quad (4.21)$$

where  $C$  is a constant independent of mesh parameters and  $\varepsilon$ . The results in Eq. (4.21) are directly derived from Eq. (4.20) and Lemma (3.1).

## 5 Numerical Results and Discussions

Computations are done for reasonable value of the free parameter  $\lambda = -0.55, 0, 0.9 \in [-8, 1]$  and  $\lambda = 0.9 \in [-8, 1]$  gives minimum error. Since the exact solution for the test example is unknown, we use the double mesh principle to calculate absolute errors. For each  $\varepsilon$ , we can determine the maximum point wise errors using the formula as

$$E_\varepsilon^{N,M} = \max_{0 \leq i, j \leq N, M} |U^{N,M}(x_i, t_j) - U^{2N, 2M}(x_{2i}, t_{2j})|,$$

where  $U^{N,M}(x_i, t_j)$  is numerical solution at  $N, M$  mesh points whereas  $U^{2N, 2M}(x_{2i}, t_{2j})$  is numerical solution at  $2N, 2M$  mesh points. The rate of convergence is calculated as:

$$R_\varepsilon^{N,M} = \log_2 \left( \frac{E_\varepsilon^{N,M}}{E_\varepsilon^{2N, 2M}} \right)$$

**Example 1.** Consider the test problem for Eq. (1.1)- (1.3)(see[24])

$$\begin{cases} x(1-x^2) \frac{\partial u}{\partial t} - \varepsilon \frac{\partial^3 u}{\partial t \partial x^2} - \varepsilon \frac{\partial^2 u}{\partial x^2} + t \sin(\pi x) u(x, t) + t^2 u(x, t-r) = \\ \quad e^{-t} \cos(t) \sin(\pi x), & (x, t) \in (0, l) \times (0, r], \\ u(x, t) = \varphi(x, t) = e^{-t} \sin(2\pi x), & (x, t) \in \bar{\Omega} \times [-r, 0], \\ u(0, t) = u(l, t) = 0, & t \in (0, T], \end{cases}$$

where  $l = 1, r = 1$  and  $T = 2$ . Here we take the value of  $\alpha = 1.25$  for all step sizes.

The computed maximum point-wise errors  $E_\varepsilon^{N,M}$  are given in Tables 2,3 and 4 for free parameter  $\lambda = 0.9, \lambda = -0.55$  and  $\lambda = 0$  respectively. From the results, it is clear that the proposed method gives an  $\varepsilon$ -uniform convergence. Table 5 displays the comparison of computational results using classical cubic B-spline method for  $\lambda = 0$  and extended B-spline method for  $\lambda = 0.9$  and  $\lambda = -0.55$ . Additionally, Table 5 provides numerical results for  $\varepsilon = 2^{-14}$  and  $N = 64, 128, 256$  that are compared to those provided in [24]. This comparison shows that the extended cubic-B-spline method on Bakhvalov mesh yields a more accurate solution when compared to studies found in [24]. Both the particular selections of the extension parameter  $\lambda$  gives numerical results, but the value of  $\lambda = 0.9$  gives better results than  $\lambda = -0.55$  and  $\lambda = 0$ . As we observe from all tables that, extended cubic B-spline have an advantage over the classical B-splines as for some optimized value of  $\lambda$ , the solution obtained by the extended B-splines is better than the solution obtained by classical B-splines. The suitable choice of the extension parameter  $\lambda$  minimizes the error. From the results in Tables 2,3 and 4, one can conclude that the computed maximum

Table 2: Maximum point-wise errors  $E_\varepsilon^{N,M}$  for various  $\varepsilon$  and  $\lambda = 0.9$ 

$\varepsilon$	$M = 16$	$M = 32$	$M = 64$	$M = 128$	$M = 256$
$\downarrow$	$N = 16$	$N = 32$	$N = 64$	$N = 128$	$N = 256$
$2^{-2}$	$2.4035e - 02$	$2.2315e - 02$	$1.5618e - 02$	$9.1187e - 03$	$4.8984e - 03$
$2^{-4}$	$2.8288e - 02$	$2.3133e - 02$	$1.5364e - 02$	$9.0625e - 03$	$4.9617e - 03$
$2^{-6}$	$3.4503e - 02$	$2.5983e - 02$	$1.6272e - 02$	$9.2397e - 03$	$4.9361e - 03$
$2^{-8}$	$3.5760e - 02$	$2.6203e - 02$	$1.6417e - 02$	$9.2191e - 03$	$4.9076e - 03$
$2^{-10}$	$3.6040e - 02$	$2.6376e - 02$	$1.6454e - 02$	$9.2113e - 03$	$4.9009e - 03$
$2^{-12}$	$3.6247e - 02$	$2.6480e - 02$	$1.6466e - 02$	$9.2050e - 03$	$4.8980e - 03$
$2^{-14}$	$3.6285e - 02$	$2.6522e - 02$	$1.6470e - 02$	$9.1994e - 03$	$4.8954e - 03$
$2^{-16}$	$3.6293e - 02$	$2.6558e - 02$	$1.6472e - 02$	$9.1954e - 03$	$4.8935e - 03$
$2^{-18}$	$3.6293e - 02$	$2.6566e - 02$	$1.6475e - 02$	$9.1941e - 03$	$4.8923e - 03$
$2^{-20}$	$3.6292e - 02$	$2.6568e - 02$	$1.6477e - 02$	$9.1932e - 03$	$4.8915e - 03$
$2^{-22}$	$3.6292e - 02$	$2.6568e - 02$	$1.6477e - 02$	$9.1932e - 03$	$4.8915e - 03$
$E_\varepsilon^{N,M}$	$3.6293e - 02$	$2.6568e - 02$	$1.6478e - 02$	$9.2397e - 03$	$4.9617e - 03$
$R_\varepsilon^{N,M}$	0.45	0.69	0.84	0.90	—

Table 3: Maximum point-wise errors  $E_\varepsilon^{N,M}$  for various  $\varepsilon$  and  $\lambda = -0.55$ 

$\varepsilon$	$M = 16$	$M = 32$	$M = 64$	$M = 128$	$M = 256$
$\downarrow$	$N = 16$	$N = 32$	$N = 64$	$N = 128$	$N = 256$
$2^{-2}$	$2.9680e - 02$	$2.7742e - 02$	$1.8708e - 02$	$1.0798e - 02$	$5.8076e - 03$
$2^{-4}$	$3.4549e - 02$	$2.8235e - 02$	$1.8596e - 02$	$1.0841e - 02$	$5.8979e - 03$
$2^{-6}$	$3.8429e - 02$	$2.9805e - 02$	$1.8916e - 02$	$1.0845e - 02$	$5.8318e - 03$
$2^{-8}$	$3.9130e - 02$	$2.9968e - 02$	$1.9044e - 02$	$1.0847e - 02$	$5.8170e - 03$
$2^{-10}$	$3.9476e - 02$	$3.0032e - 02$	$1.9086e - 02$	$1.0845e - 02$	$5.8091e - 03$
$2^{-12}$	$3.9618e - 02$	$3.0053e - 02$	$1.9106e - 02$	$1.0841e - 02$	$5.8036e - 03$
$2^{-14}$	$3.9643e - 02$	$3.0093e - 02$	$1.9113e - 02$	$1.0838e - 02$	$5.7994e - 03$
$2^{-16}$	$3.9643e - 02$	$3.0105e - 02$	$1.9114e - 02$	$1.0836e - 02$	$5.7965e - 03$
$2^{-18}$	$3.9637e - 02$	$3.0108e - 02$	$1.9125e - 02$	$1.0835e - 02$	$5.7948e - 03$
$2^{-20}$	$3.9631e - 02$	$3.0107e - 02$	$1.9128e - 02$	$1.0835e - 02$	$5.7943e - 03$
$2^{-22}$	$3.9631e - 02$	$3.0107e - 02$	$1.9128e - 02$	$1.0835e - 02$	$5.7943e - 03$
$E_\varepsilon^{N,M}$	$3.9643e - 02$	$3.0108e - 02$	$1.9128e - 02$	$1.0847e - 02$	$5.8979e - 03$
$R_\varepsilon^{N,M}$	0.40	0.66	0.82	0.88	—

point-wise error decreases as  $N$  increases for each value of  $\varepsilon$ . To see the effect of delay and extension parameter  $\lambda$  in the boundary regions, graphs are plotted on the solution profiles for  $\lambda \in [-8, 1]$ . Figures 1(a) and 1(b) depicts the numerical simulation of solution profile at  $N = M = 128, \varepsilon = 2^{-8}, \lambda = -0.55$  and  $N = M = 128, \varepsilon = 2^{-8}, \lambda = 0.9$  respectively, which indicates parabolic boundary layers at  $x = 0$  and  $x = 1$ . Figures 2(a) and 2(b) are the

Table 4: Maximum point-wise errors  $E_\varepsilon^{N,M}$  for various  $\varepsilon$  and  $\lambda = 0$ 

$\varepsilon$	$M = 16$	$M = 32$	$M = 64$	$M = 128$	$M = 256$
$\downarrow$	$N = 16$	$N = 32$	$N = 64$	$N = 128$	$N = 256$
$2^{-2}$	$2.7202e - 02$	$2.5288e - 02$	$1.7421e - 02$	$1.0097e - 02$	$5.4264e - 03$
$2^{-4}$	$3.1892e - 02$	$2.6085e - 02$	$1.7243e - 02$	$1.0092e - 02$	$5.5085e - 03$
$2^{-6}$	$3.6842e - 02$	$2.8227e - 02$	$1.7818e - 02$	$1.0174e - 02$	$5.4512e - 03$
$2^{-8}$	$3.7795e - 02$	$2.8423e - 02$	$1.7954e - 02$	$1.0168e - 02$	$5.4356e - 03$
$2^{-10}$	$3.8103e - 02$	$2.8473e - 02$	$1.7999e - 02$	$1.0163e - 02$	$5.4269e - 03$
$2^{-12}$	$3.8283e - 02$	$2.8503e - 02$	$1.8014e - 02$	$1.0158e - 02$	$5.4208e - 03$
$2^{-14}$	$3.8321e - 02$	$2.8548e - 02$	$1.8020e - 02$	$1.0153e - 02$	$5.4167e - 03$
$2^{-16}$	$3.8319e - 02$	$2.8582e - 02$	$1.8021e - 02$	$1.0151e - 02$	$5.4135e - 03$
$2^{-18}$	$3.8319e - 02$	$2.8590e - 02$	$1.8029e - 02$	$1.0150e - 02$	$5.4114e - 03$
$2^{-20}$	$3.8315e - 02$	$2.8592e - 02$	$1.8031e - 02$	$1.0149e - 02$	$5.4107e - 03$
$2^{-22}$	$3.8315e - 02$	$2.8592e - 02$	$1.8031e - 02$	$1.0150e - 02$	$5.4107e - 03$
$E_\varepsilon^{N,M}$	$3.8321e - 02$	$2.8592e - 02$	$1.8031e - 02$	$1.0174e - 02$	$5.5085e - 03$
$R_\varepsilon^{N,M}$	0.43	0.67	0.83	0.89	—

Table 5: Comparison of maximum point-wise errors with results in [24].

	$(N, M) = 16$	$(N, M) = 32$	$(N, M) = 64$	$(N, M) = 128$	$(N, M) = 256$
For $\lambda = -0.55$					
$E_\varepsilon^{N,M}$	$3.9643e - 02$	$3.0108e - 02$	$1.9128e - 02$	$1.0847e - 02$	$5.8979e - 03$
$R_\varepsilon^{N,M}$	0.40	0.66	0.82	0.88	—
For $\lambda = 0$					
$E_\varepsilon^{N,M}$	$3.8321e - 02$	$2.8592e - 02$	$1.8031e - 02$	$1.0174e - 02$	$5.4512e - 03$
$R_\varepsilon^{N,M}$	0.43	0.67	0.83	0.89	—
For $\lambda = 0.9$					
$E_\varepsilon^{N,M}$	$3.6293e - 02$	$2.6568e - 02$	$1.6478e - 02$	$9.2397e - 03$	$5.5085e - 03$
$R_\varepsilon^{N,M}$	0.45	0.69	0.84	0.90	—
Present Method for $\epsilon = 2^{-14}, N = 64, 128, 256$					
$E^{N,M}$			$1.6470e - 02$	$9.1994e - 03$	$4.8954e - 03$
Results presented in [24] for $\epsilon = 2^{-14}, N = 64, 128, 256$					
$E^{N,M}$			$2.1473e - 01$	$1.0858e - 01$	$2.9661e - 02$

numerical simulations of the solution profile using line graph at  $N = M = 64, \varepsilon = 2^{-6}, \lambda = 0.9$  and with different time level for  $N = M = 64, \varepsilon = 2^{-6}, \lambda = 0.9$  respectively. We see that from Figures 2(a) and 2(b), when  $\varepsilon \rightarrow 0$  strong boundary layer is formed near the neighborhood of  $x = 0$  and  $x = 1$ . The maximum point-wise error values are plotted using Log-Log scale for  $\lambda = -0.55, \lambda = 0$  and  $\lambda = 0.9$  in figure 3. Figure 4(a) depicts the numerical simulation profile for  $N = M = 256, \varepsilon = 2^{-12}, \lambda = 0$  by using mesh plot. Figure 4(b) depicts the numerical simulation profile for  $N = M = 256, \varepsilon = 2^{-12}, \lambda = -0.55$  using surface plot with highlights from a light

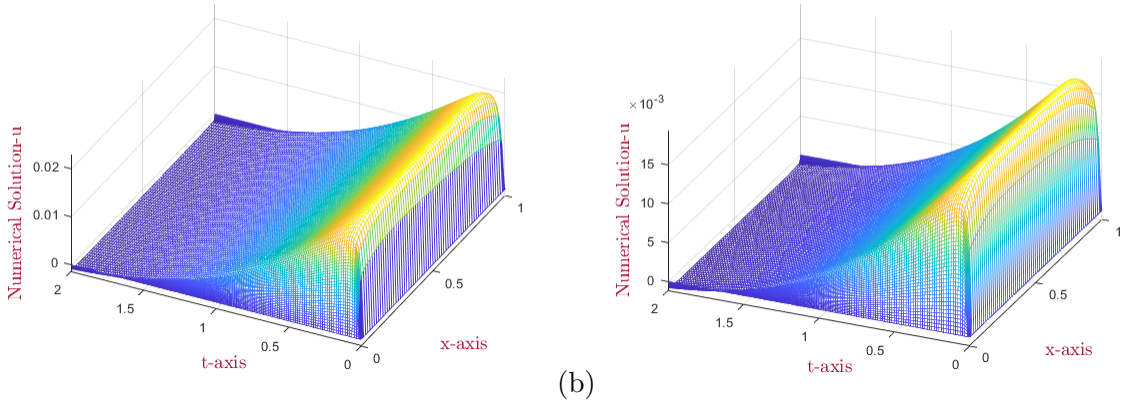


Figure 1: Numerical solution profiles for (a)  $N = 128, M = 128, \varepsilon = 2^{-8}, \lambda = -0.55$  and (b)  $N = 128, M = 128, \varepsilon = 2^{-8}, \lambda = 0.9$  respectively.

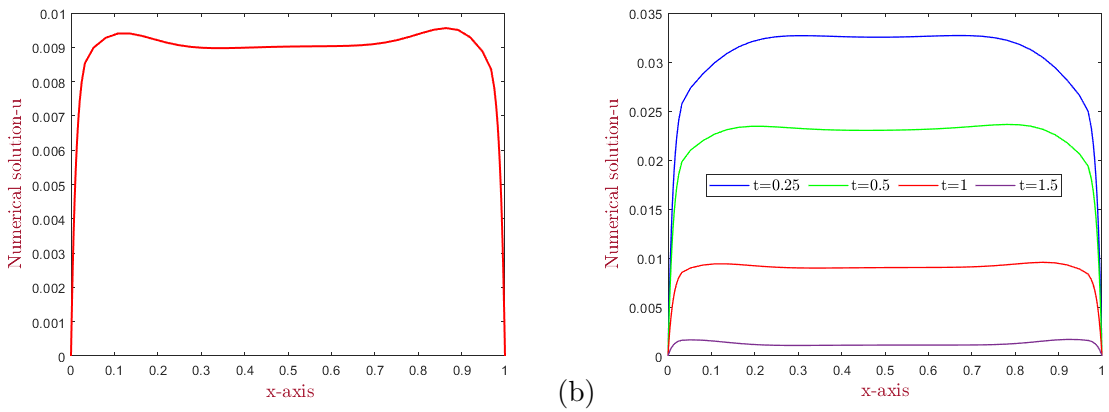


Figure 2: The behavior of spatial vs numerical solution graph: The left is Line graph and with different time level on the right at  $N = M = 64, \varepsilon = 2^{-6}, \lambda = 0.9$  respectively

source. As one can observe from Figure 4(a) and (b), strong boundary layer is formed at  $x = 0$  and  $x = 1$ .

## 6 Conclusion

In this work, a parameter uniform numerical scheme has been developed to find approximate solution of singularly perturbed delay Sobolev problems. The proposed method is based on Implicit-Euler scheme for time derivative on uniform mesh and the extension of cubic B-spline with a blending function of degree four in the spatial direction on Bakhvalov type mesh. With flexibility of extensions, the approximations of the solution can be made more accurate by adjusting the free parameter  $\lambda$ . The method is shown to be first-order accurate with respect to time and second-order accurate with respect to spatial direction. A single example has been provided, and the results are displayed using MATLAB software in tables and graphs to validate the theoretical

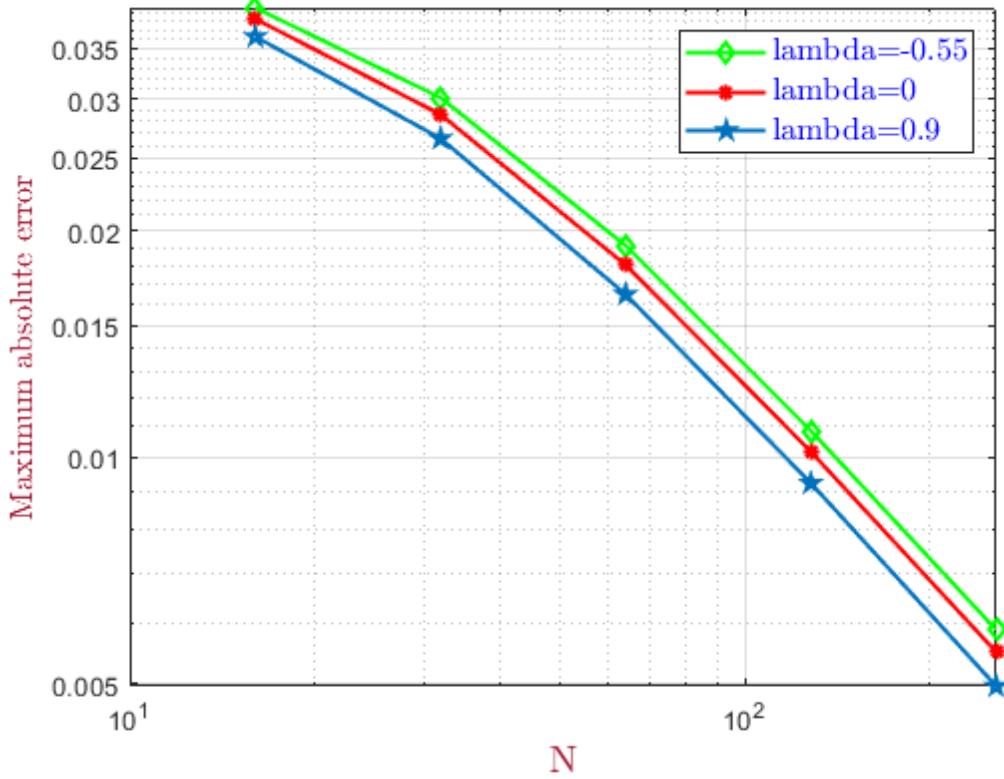


Figure 3: Plot of maximum absolute errors in log-log for  $\lambda = 0$ ,  $\lambda = -0.55$  and  $\lambda = 0.9$ .

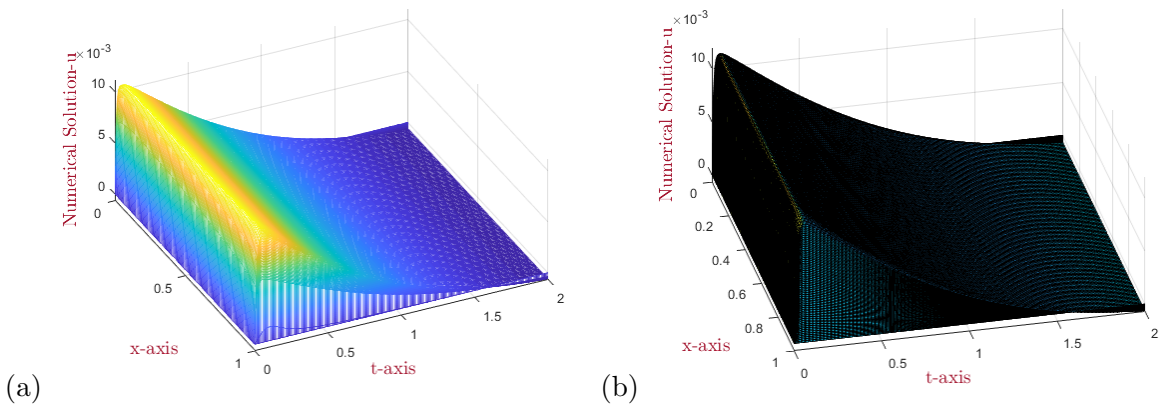


Figure 4: Numerical solution profiles using mesh plot and using surface plot for (a)  $N = 256 = M, \varepsilon = 2^{-12}, \lambda = 0$  and (b)  $N = 256 = M, \varepsilon = 2^{-12}, \lambda = -0.55$  respectively.

convergence results and show the applicability of the suggested method. The numerical example confirms the theoretical analyses. The developed method can be used as an alternative method

for similar and related Sobolev problems.

## Acknowledgments

The authors are grateful to the anonymous reviewers for their valuable comments in the improvement of this manuscript. There is no supported body to do this research.

**Disclosure Statement:** The authors reported no potential conflicts of interest.

## References

- [1] A.B. Vasilieva, Asymptotic methods in the theory of ordinary differential equations containing small parameters in front of the higher derivatives, *USSR Comput. Math. & Math. Phys.*, **3**(1963),823–863.
- [2] S.L. Cheru, G.F.Duressa, and T.B.Mekonnen, Numerical integration method for two-parameter singularly perturbed time delay parabolic problem, *Front. Appl. Math. Stat.*,**10**(2024),1414899.
- [3] G. M. Amiraliyev & Y. D. Mamedov, Difference schemes on the uniform mesh for SP pseudo-parabolic equations, *Turkish Jou.of Math.*, **19**(3)(1995), 207–222.
- [4] A. B. Chiyaneh, & H. Duru, On adaptive mesh for the initial boundary value singularly perturbed delay Sobolev problems. *Numer. Methods for PDEs*, **36**(2)(2020),228–248.
- [5] A. B. Chiyaneh, &H. Durus, Uniform difference method for SP delay Sobolev problems. *Quaestiones Mathematicae*, **43**(12)(2020), 1713–1736.
- [6] H. Duru, Difference schemes for the singularly perturbed Sobolev periodic boundary problem, *Appl. math. and comput.*, **149**(1)(2004), 187–201.
- [7] C. Clavero, J. Jorge & F. Lisbona, Uniformly convergent schemes for SPPS combining alternating directions and exponential fitting techniques, *Appliat. avanc. comput. methods for boundary and interior layers*,(1993) pages 33–52.
- [8] I. T. Daba and G. F. Duressa, Extended cubic B-spline collocation method for SPP differential-difference equation arising in computational neuroscience. *I. J. Numer. methods in biome. engin.*, **37**(2)(2021), e3418.
- [9] F. W. Gelu, and G. F.Duressa, A uniformly convergent collocation method for singularly perturbed delay parabolic reaction-diffusion problem, *Abstr. Appl. Anal*, pp.,(2021, March),1–11,
- [10] D.Kumar and P.Kumari, A parameter-uniform scheme for singularly perturbed partial differential equations with a time lag, *Numer. Methods Partial. Differ. Equ.*, **36**(4)(2020), 868–886 .
- [11] T.C.Hall, On error bounds for spline interpolation. *J. Approx. Theory*, **1**(2)(1968),209–218.
- [12] M. Amrein & T. P. Wihler, An adaptive space-time Newton Galerkin approach for semilinear singularly perturbed parabolic evolution equations. *MA J. Numer. Anal.*, **37**(4)(2017), 2004–2019.

- 
- [13] R. E. Ewing, Numerical solution of Sobolev partial differential equations, *SIAM J. Numer. Anal.*, **12**(3)(1975), 345-363.
- [14] H. Gu, Characteristic finite element methods for nonlinear Sobolev equations, *Appl. Math. Comput.*, **102**(1)(1999), 51-62.
- [15] I. Amirali, Analysis of higher order difference method for a pseudo-parabolic equation with delay, *Miskolc Math. Notes*, **20**(2)(2019), 755-766.
- [16] I. Amirali & G. M. Amiraliyev, Three layer difference method for Sobolev equation with delay, *J. Comput. Appl. Math.*, **401**(2022), 113786.
- [17] G. M. Amiraliyev, E. Cimen, I. Amirali & M. Cakir, High-order finite difference technique for delay pseudo-parabolic equations, *J. Comput. Appl. Math.*, **321**(2017), 1-7.
- [18] C. Zhang and Z. Tan, Linearized compact difference methods combined with Richardson extrapolation for nonlinear delay Sobolev equations, *Commun. Nonlinear. Sci. Numer. Simul.*, **91**(2020), 105461.
- [19] N. H. Nhan, T. T. M. Dung, L. T. M. Thanh, L. T. P. Ngoc, and N. T. Long, A High-Order Iterative Scheme for a Nonlinear Pseudo parabolic Equation and Numerical Results, *Math. Probl. Eng.*, **2021**(2021), 1-17.
- [20] H. Di, Y. Shang & X. Zheng, Global Well-Posedness for a Fourth Order Pseudo-Parabolic Equation with source term, *Disc. Cont. Dyn-S*, **21**(3)(2016).
- [21] P. Farrell, A. Hegarty, J. M. Miller, E. O'Riordan, and G. I. Shishkin, *Robust computational techniques for boundary layers*. CRC Press(2000).
- [22] G. M. Amiraliyev, H. Duru, & I. G. Amiraliyeva, A parameter-uniform method for a Sobolev problem with initial layer, *Numerical Alg.*, **44**(2007), 185-203.
- [23] B. Gunes, and H. Duru, A second-order difference scheme for the singularly perturbed Sobolev problems with third type boundary conditions on Bakhvalov mesh, *J. differ. equ. appl.*, **28**(3)(2022), 385-405.
- [24] B. Gunes and H. Duru, A computational method for singularly perturbed delay pseudo-parabolic Des on adaptive mesh, *Int. J. Comput. Math.*, **1-16**(2023).
- [25] D. Arslan, A New Error Evaluation for Singularly Perturbed Problem with Multi-Point Boundary Condition. *Comput. Methods for DEs*, **8**(2)(2020), 236-250.

**Shegaye Lema Cheru** Department of Mathematics, Wollega University, Ethiopia

E-mail: [shegaye04@gmail.com](mailto:shegaye04@gmail.com)

**Gemechis File Duressa** Department of Mathematics, Jimma University, Ethiopia

E-mail: [gammeef@gmail.com](mailto:gammeef@gmail.com)

**Tariku Birabasa Mekonnen** Department of Mathematics, Wollega University, Ethiopia

E-mail: [seena29@gmail.com](mailto:seena29@gmail.com)